Proceedings of the 21st ICSMGE, Vienna, Austria, 14 – 19 June 2026. Pistrol, Adam & Schweiger (eds.)
Published by: ÖGG, Austrian Society for Geomechanics, Salzburg, Austria, ISBN 978-3-9503898-4-5
https://doi.org/10.53243/ICSMGE2026-198

Modeling spatial variability of jet grouting columns

Stefano Collico
Department of Civil and Environmental Engineering, Universitá degli Studi di Firenze, Italy

Giovanni Spagnoli
Sweco GmbH, Germany, giovanni.spagnoli@sweco-gmbh.de

ABSTRACT: Jet grouting is widely used for ground improvement, yet its design remains affected by substantial uncertainty in both geometric and mechanical parameters, particularly the unconfined compressive strength (UCS) of the treated soil. These uncertainties become more predominant in heterogeneous soil deposits, where different combinations of jetting parameters might be selected to meet minimum design requirements. This study introduces a hierarchical Gaussian Process (GP) with non-Gaussian likelihood to model the spatial variability of UCS in jet-grouted soils. The methodology integrates three levels of information: (i) a global Gaussian Process with Weibull likelihood; (ii) geology-specific GP formulated through hierarchical priors; and (iii) a target site-level random-effect that updates the latent GP predictions as new target site UCS measurements become available. The hierarchical formulation allows the model to share information among geologically related sites, improving statistical significance when data are limited, while still accommodating site-specific spatial variability. This results in principled Bayesian updating of UCS predictions under sparse observations and yields design-ready estimates with quantified uncertainty. The proposed framework is applied to a published case study involving the Rapid-Jet system in soft marine clay, demonstrating significant improvements in predictive accuracy and reliability compared with non-hierarchical alternatives.

KEYWORDS: Jet grouting, Hierarchical Gaussian process, Weibull likelihood, Unconfined Compressive Strength.

1 INTRODUCTION

Jet grouting is a widely adopted ground-improvement technique used for foundation reinforcement, settlement mitigation, and stabilization of excavations and tunnels (e.g., Croce et al., 2014; Toraldo et al., 2017; Spagnoli & Oreste, 2025). The method consists of injecting a high-velocity water–cement mixture or other fluids into the ground to form cylindrical cemented bodies, commonly referred to as jet-grouted columns. Modern systems are generally classified into single-fluid, double-fluid, and triple-fluid configurations depending on the number of fluids involved. Several technological developments over the past two decades have focused on optimizing column dimensions and improving the mechanical performance of the treated soil (Shibazaki, 2003).

Despite these advances, predicting jet-grouted column diameter and unconfined compressive strength (UCS) based on geological description and indirect geotechnical information (e.g., Standard Penetration Test values, N_{SPT}) remains highly challenging. Several theoretical, empirical, and semi-empirical models have been proposed to estimate column dimensions (Modoni et al., 2006; Ribeiro & Cardoso, 2017). Theoretical formulations based on fluid–soil interaction (Ho, 2007) are rigorous but require parameters that are often poorly constrained in practice, while empirical models might suffer from limited data availability and site applicability.

Predicting UCS is even more challenging. Parametric regression methods, such as those discussed by Yoshida et al. (2021) and Collico et al. (2023), have been proposed by Zhao et al. (2023) and Akan et al. (2015), who applied such models to estimate unconfined compressive strength with promising accuracy. Nevertheless, these methods remain rarely employed and rely on parametric assumptions, which can limit their applicability when datasets are limited, noisy, or do not conform to assumed distributions.

Current research relies increasingly on black-box, machine-learning models (Tinoco et al. 2014), which can capture nonlinear trends but provide only point predictions and do not elicit the aleatory and epistemic uncertainty involved. Furthermore, models trained on global (i.e. generic) databases often perform poorly when applied to new target sites with different geological and geotechnical characteristics (Ching et al. 2021). Ideally, jet grouting design would rely on local predictive models calibrated using site-specific UCS measurements. However, jet grouting projects typically provide only a small number of UCS tests per site, often limited to quality-control cores. This scarcity of data makes purely local modeling statistically unreliable and leads to substantial uncertainty in early design stages.

To address these challenges, this study develops a hierarchical Gaussian Process (GP) regression model with a Weibull likelihood for predicting the UCS of jet-grouted columns. Unlike a Gaussian likelihood, the Weibull formulation enables flexible modelling of the positively skewed, heavy-tailed behavior characteristic of UCS data, thereby substantially increasing modelling flexibility. The proposed model explicitly quantifies epistemic uncertainty and allows hierarchical predictions to be updated as new observations become available. The hierarchical structure is composed of three levels: a global GP with Weibull likelihood; geology-specific GPs introduced through hierarchical priors that pool statistical strength across similar lithologies; and a site-level depth-dependent GP that refines predictions using local UCS data. This approach allows fully probabilistic UCS estimates and enables principled Bayesian updating. Validation using a published Rapid-Jet case study in marine clay demonstrates notable gains in predictive performance compared with hierarchical models that are not updated with target-site measurements.

2 DATASET OVERVIEW

The database used in this study is an extended version of the one presented by Collico et al. (2025), which was initially compiled for double-fluid jet grouting systems including only jet-column diameters and UCS values across project sites in Japan. For each site, mean estimate of jet grouting system's parameters and Standard Penetration Test value (N_{SPT}) are available, together with multiple UCS measurements. The dataset comprises: soil classification, Standard Penetration Test value (N_{SPT}), grout pressure, grout flow rate, water/cement ratio, rotation speed, lifting speed, jet-column diameter, and UCS.

An overview of the parameters involved is shown in Figure 1, which reveals complex pairwise dependencies among jet grouting parameters, UCS, and N_{SPT} values. Such complex dependence underscores the need for a flexible, multi-level statistical model capable of capturing both global patterns and site-specific deviations.

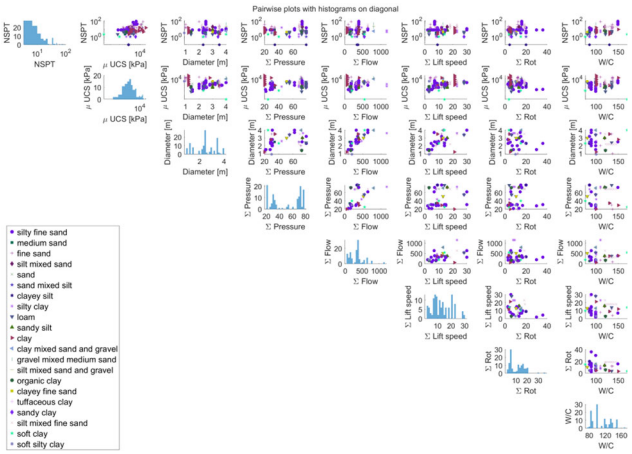

Figure 1. Pairwise data scatter of compiled dataset.

3 METHODOLOGY

The objective of this work is to develop a probabilistic framework capable of predicting the unconfined compressive strength (UCS) of jet-grouted columns at a target site while: (i) quantifying uncertainty; (ii) exploiting information from a multi-site database; and (iii) allowing for site-specific updating when local UCS tests become available. To achieve this, a hierarchical Gaussian Process (GP) with non-Gaussian likelihood is introduced. A simplified overview of the hierarchical structure is reported in Figure 2. The method combines:

1. A global, Weibull-GP regression.
2. Geology-specific GPs, whose hyperparameters are partially pooled toward the global hyperparameters through hierarchical priors.
3. A site-level updating using a depth-GP random effect, to integrate target site UCS measurements.

The adoption of geology-specific GPs represents a pragmatic form of dataset clustering, justified by the structure and volume of the currently available database (i.e. for each site a single mean estimate of each parameter, except for UCS, is available). Other clustering strategies—such as grouping by jetting fluid system (e.g., Díaz et al., 2024) or by geotechnical and/or statistical characteristics (Wu et al., 2022, Collico et al., 2023)—could, in principle, be incorporated within the same hierarchical framework. However, these alternatives require richer and more comprehensive datasets and are therefore left for future extensions of this work.

Concerning the selected statistical model, the Weibull model is employed due to its flexibility in capturing the empirical distribution of geology-specific UCS. As shown in Figure 3, the marginal distributions of UCS exhibit right-skewness, and non-constant dispersion across soil types—features that might not be adequately represented by Gaussian models. The Weibull distribution, through its independent shape and scale parameters, adapts naturally to these changes in skewness and tail behavior. Figure 3 provides supporting evidence for the Weibull choice, showing marginal kernel-density estimates and fitted Weibull probability density functions for UCS and N_{SPT}, across the three geological clusters considered.

The formulation follows the general treatment of GP models with arbitrary differentiable likelihoods described by Murphy (2023), implemented via Laplace approximation. Although other positive-valued likelihoods (e.g., gamma, lognormal) could be embedded in the same GP formulation, their comparative performance, model averaging, and adaptive likelihood selection remain outside the scope of this study.

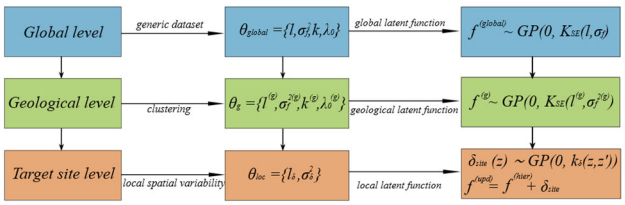

Figure 2. Hierarchical structure of proposed methodology.

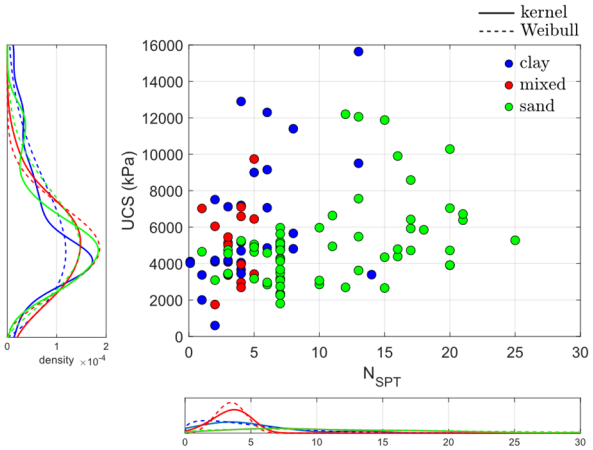

Figure 3. Scatter, kernel density and Weibull density fit to dataset employed.

3.1 *Global level*

Let X denote the covariates for generic sites (injected pressure, lift speed, rotation speed, N_{SPT} value, water/cement ratio) and let Y = UCS denote the measured UCS. At the global level UCS observations are assumed to fit a Weibull regression model such that:

$$Y \mid f, k \sim Weibull(k, \lambda_0 \, e^{f}) \tag{1}$$

with k global Weibull shape parameter, λ_0 global scale coefficient and f=f(X) latent log-scale function. A GP prior is placed on $f(\cdot)$ such that (Murphy, 2023):

$$f(\cdot) \sim \mathcal{GP}(0, k_{\mathrm{SE}}(\cdot, \cdot \,; \ell, \sigma_f^2)) \tag{2}$$

with k_{SE} autocovariance matrix (Yoshida et al., 2021). In this study the isotropic squared-exponential kernel is assumed for simplicity which reads:

$$k_{\mathrm{SE}}(x, x') = \sigma_f^2 \exp\left(-\frac{\| x - x' \|^2}{2\,\ell^2}\right) \tag{3}$$

with σ_f^2, ℓ global variance and scale of fluctuation respectively.

Thus, the global parameter array, defined as $\theta_{\mathrm{global}} = \{\ell, \sigma_f^2, k, \lambda_0\}$, characterizes the global level. Because the Weibull likelihood is non-Gaussian, the posterior over f does not admit a closed-form solution. Following standard Gaussian-process regression for non-Gaussian likelihoods, a Laplace

approximation is required. The global parameters are then estimated by maximizing the approximate marginal likelihood described in Rasmussen & Williams, (2006), Nickisch & Rasmussen, (2008):

$$\hat{\theta}_{\text{global}} = \arg\max_{\theta_{\text{global}}} \big(logp(Y|\, X, \theta_{\text{global}})\big) \tag{4a}$$

Using the Laplace approximation, this becomes:

$$\hat{\theta}_{\text{global}} \approx arg\max_{\theta} [logp(Y\,|f^*(\theta), \theta) - 0.5 \log\,(detA(\theta))] \tag{4b}$$

with $f^*(\theta)$is the Laplace mode (i.e., the MAP estimate) of the latent function and $A(\theta)$is the negative Hessian of the log-posterior with respect to f.

3.2 *Geologic level*

Sites in the dataset are grouped into three coarse geological classes: clay, mixed soil, and sand. For each class g, geology-specific GP (Equation 5a) and Weibull regression model (Equation 5b) are considered such that:

$$f^{(g)}(\cdot) \mid \theta_g \sim \mathcal{GP}(0, k_{SE}^{(g)}(\cdot\,,\,\cdot\,;\,\ell^{(g)}, \sigma_f^{2(g)})) \tag{5a}$$

$$Y^{(g)} \mid f_i^{(g)}, k_g, \lambda_{0,g} \sim \text{Weibull}(k^{(g)}, {\lambda_0}^{(g)} e^{f^{(g)}}) \tag{5b}$$

Therefore, each geological level has its own covariance structure—through $l^{(g)}$(length scale) and $\sigma_f^{2(g)}$(latent variance)—and its own Weibull shape $k^{(g)}$and scale coefficient $\lambda_0^{(g)}$ such that $\theta_g = (\ell^{(g)}, \sigma_f^{2(g)}, k^{(g)}, {\lambda_0}^{(g)})$. To prevent overfitting—given that per-class data may be limited—a partial pooling by shrinking geology-level parameters toward global parameters is introduced such that:

$$\theta_g = \theta_{\text{global}} \odot \exp\,(\delta_g) \text{ with } \delta_g \sim \mathcal{N}(0, \text{diag}(\tau_g^2)) \tag{6}$$

where $\odot$ denotes element-wise multiplication. The parameter $\tau_g$controls the deviation of θ_g from the global parameters: small $\tau_g$enforces strong shrinkage toward θ_{global}, while larger τ_g permits geology-specific differences when supported by the data.

Geological-specific hyperparameter θ_g are then obtained by maximizing a penalized Laplace–approximate marginal likelihood:

$$\begin{aligned}\hat{\theta}_{\text{g}} = \arg\max_{\theta_{\text{g}}} \Big[&\big(\log p_{Lap}\,\big(Y_g\big|\, X_g, \theta_{\text{g}}\big) \\ &- 0.5\big(\log\theta_{\text{g}} \\ &- \log\theta_{\text{global}}\big)^T \,\text{diag}(\tau_g^{-2})\big(\log\theta_{\text{g}} \\ &- \log\theta_{\text{global}}\big)\Big]\end{aligned} \tag{7}$$

3.3 *Hierarchical latent predictor*

For any new input X, both the global and the geological model yield Gaussian latent approximation:

$$f^{(global)} \sim\ N(\mu_{global}(X), \sigma_{global}^2(X)) \tag{8a}$$

$$f^{(g)} \sim\ N(\mu_g(X), \sigma_g^2(X)) \tag{8b}$$

They are combined using precision weighting giving the hierarchical predictor such that (Zhang et al. 2004; Ang & Tang, 2007):

$$f^{(\text{hier})} \sim\ N(\mu_{\text{hier}}(X), \sigma_{hier}^2(X)) \tag{8c}$$

$$\mu_{\text{hier}}(X) = \frac{\tau_{glob}(X)\,\mu_{\text{global}}(X) + \tau_g(X)\,\mu_{\text{cluster}}(X)}{\tau_{glob}(X) + \tau_g(X)} \tag{8d}$$

$$\tau_{glob}(X) = \frac{1}{\sigma_{global}^2(X)};\ \tau_g(X) = \frac{1}{\sigma_g^2(X)} \tag{8e}$$

$$\sigma_{hier}^2(X) = \big(\tau_{\text{global}}(X) + \tau_{\text{g}}(X)\big)^{-1} \tag{8f}$$

This provides intuitive behavior: high-uncertainty geological clusters borrow strength from the global model, whereas data-rich clusters rely on their own geology-specific GP.

Finally, the hierarchical latent predictor controls the Weibull scale parameter for UCS distribution at input X belonging to geology g:

$$\text{UCS}(x) \mid f(X) \sim \text{Weibull}\,(k^{(g)}, {\lambda_0}^{(g)} e^{f^{(hier)(X)}}) \tag{9}$$

3.4 *Target site Updating*

Even after conditioning on the global and geology-specific GPs, a new target site j, typically exhibits systematic discrepancies between the hierarchical GP predictions and target site UCS trend. These discrepancies may reflect changes in chemo-physical soil conditions, construction quality, or unobserved heterogeneities. To account for this, a site-level random effect $\delta_{\text{site}}(z)$ acting on the latent log-scale function of the Weibull model is considered. For a depth z_j at the target site, the local UCS is again modeled by Weibull model such as:

$$Y_j \sim \text{Weibull}(k^{(g)}, {\lambda_0}^{(g)} e^{f(z_j)}) \tag{10a}$$

with $f(z_j)$ latent field:

$$f(z_j) = f^{(\text{hier})}(z_j) + \delta_{\text{site}}(z_j) \tag{10b}$$

where $f^{(\text{hier})}(z_j)$ prediction computed according to Equation (8c) by considering covariate X at depth z_j.

The local effect is modeled as a one-dimensional Gaussian process along depth, $\delta_{\text{site}}(z) \sim GP\big(0, k_\delta\,(z, \text{z}')\big)$ with $k_\delta\,(z_j, {z_j}')$ squared exponential autocovariance matrix with scale length ℓ_δ and variance σ_δ^2 both learned from data residuals at target site.

Residuals relative to the hierarchical predictor are computed as:

$$r_j\ =\ \log\ \Big(\frac{Y_j}{{\lambda_0}^{(g)}}\Big)\ -\ f^{(\text{hier})}(z_j) \tag{11}$$

These residuals are treated as noisy observations of the latent depth-varying deviation. Performing GP regression on pairs $\{(z_j, r_j)\}$ yields the posterior mean $\delta_{\text{mean}}(z)$ and posterior variance $\delta_{\text{var}}(z) = \sigma_{loc}^2$. The posterior (i.e. updated) latent function at the target site is obtained by correcting the hierarchical predictor with the inferred site-specific deviation such as (Deisenroth & Ng, 2015):

$$\begin{aligned} &f^{(\text{upd})}\big(z_j\big) \\ &=\ \frac{\sigma_{hier}^{-2}\big(z_j\,\big) f^{(\text{hier})}\big(z_j\big) + \sigma_{loc}^{-2}\,(z_j)\delta_{\text{mean}}(z_j)}{\sigma_{hier}^{-2} + \sigma_{loc}^{-2}} \end{aligned} \tag{12a}$$

$$\sigma_{upd}^2 = \big(\sigma_{hier}^{-2}\big(z_j\,\big) + \sigma_{loc}^{-2}\,(z_j)\big)^{-1} \tag{12b}$$

with σ_{upd}^2 updated variance. Thus, the final local latent function respects the global and geological structure while adapting flexibly to local spatial variability.

4 HIERARCHICAL MODEL VALIDATION

Global and geology-specific hyperparameters are learned from the compiled dataset through maximization of the penalized Laplace–approximate marginal likelihood according to Eq. (4b) and Eq. (7). As an illustration, Figure 4a reports the pairwise posterior scatter plots for global $\hat{\theta}_{\text{global}}$, and geological $\hat{\theta}_{\text{g}}$ hyperparameters. These visual diagnostics reveal how the global and geological Weibull shape, scale coefficient, and GP kernel parameters co-vary when fitted to the dataset.

The hierarchical model's predictive performance, evaluated through site-level K-fold cross-validation, is reported in Figure 4b. Predictions are expressed as posterior means together with 95% predictive intervals. The hierarchical GP achieves relatively strong accuracy, with R^2 of about 0.78 across folds, and a minor difference during K-fold training (R^2=0.73). The uncertainty bands behave consistently with the database distribution: they are relatively narrow in well-represented regions of the covariate space and widen in sparse areas, reflecting increased epistemic (i.e. statistical and transformation model) uncertainties.

Figure 4b also suggests that the dataset is likely reliable for UCS values greater than 2000 kPa, while lower values might be overpredicted due to the lack of sufficient information in the dataset.

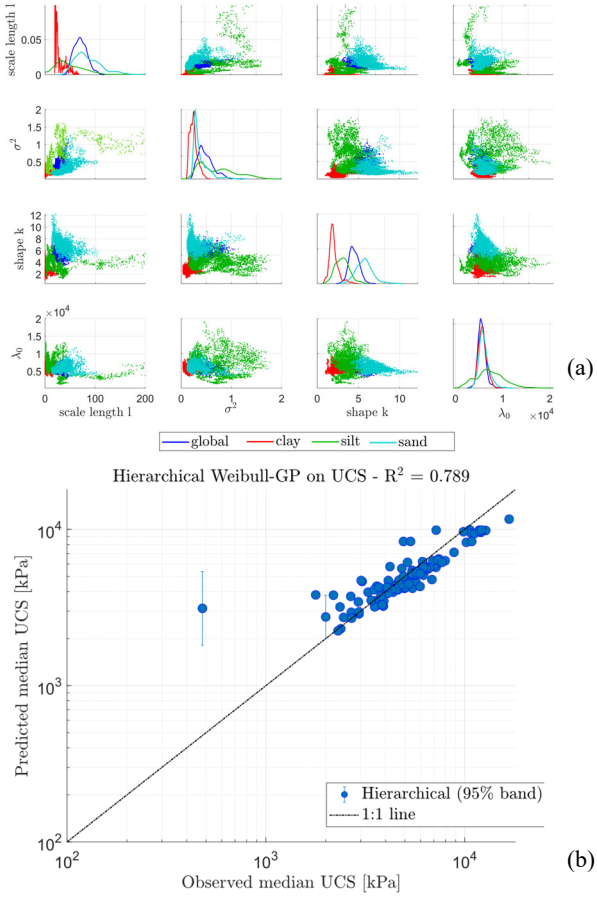

Figure 4. a) Data scatter of learned global and geological hyperparameters. b) Prediction capability of Hierarchical GP for Weibull regression.

5 CASE STUDY

The proposed methodology is applied to a case study that concerns the Rapid-Jet system for installation of jet grout piles (JGP) in soft marine clay of up to 44.8 m (Iwakubo et al., 2019), which was part of the ground improvement works for the construction of one of the tunnelling projects constructed by China Railway First Group Co. Ltd. Singapore Branch in Singapore. The large diameter JGPs served 2 purposes: 1) to mechanically improve the soft marine clay and 2) to grout to the bottom of the storm water pipe. The average grout depth was 37 m, and the average drill depth was 45 m. The geological soil profile is reported in Figure 5a. The stratigraphy consists of five primary units. The "Sand Fill Layer" extends from 0 to 14.5 m depth and is composed of fine- to coarse-grained sand with gravel, exhibiting N_{SPT} values ranging from 3 to 16. The "Soft Marine Clay" unit, part of the Kallang Formation, spans from 14.5 to 23 m depth and displays low stiffness and high compressibility. Below this lies the "Stiff Fluvial Clay" layer, also within the Kallang Formation (F2 subunit), extending from 23 to 28.7 m depth with N_{SPT} values of 8–9. A deeper "Very Soft Marine Clay" unit within the Kallang Formation reaches a depth of about 44.8 m, characterized by markedly reduced shear strength. Finally, the "Old Alluvium" unit, consisting of medium-dense to dense cemented clayey sand, extends beyond 44.8 m depth and shows N_{SPT} values of 24–36. UCS laboratory measurements collected within a 4.5 m radius (Figure 5b) reveal significant strength variability in jet columns. Observed jet-column diameters range between 3.0 m and 3.5 m, consistent with typical grouting outcomes for such heterogeneous strata.

5.1 *Unconfined Compressive Strength Prediction*

To illustrate the benefit of proposed hierarchical updating, four case scenarios are considered by accounting for a different amount of target-site information:

A. No local information
B. 15% of local information
C. 30% of local information
D. 90% of local information

Scenario A represents the early, preliminary design phase, where only the geological description of the site, in-situ tests (N_{SPT}), and the planned jet grouting system are available. Under these conditions, UCS predictions rely entirely on the hierarchical model trained on the compiled database.

The geological description, shown in Figure 5a, is used to uniquely assign each depth to one of the geological clusters g. The corresponding predictions are reported in Figure 6a. Blue markers denote local UCS measurements, which in this scenario are used only for validation. The dashed curve shows the median UCS profile obtained from the combined global and geology-specific GPs, while the shaded band represents the associated 95% confidence interval. Results clearly indicate a tendency to overestimate UCS with depth. This overestimation is not unexpected: the compiled database contains many cases with relatively high UCS, which biases the hierarchical prediction. The large uncertainty region further reflects that the covariates X at the target site depth lie in regions of the input space that are sparsely represented in the training data.

Scenario B (15% local data, Figure 6b), introduces a very small fraction of local UCS measurements (i.e. 3 data points). Due to the limited local information, the posterior UCS profile undergoes a slight update, especially in the posterior median. This behavior stems from the model's structure: the hierarchical GP provides a prior trend, whereas the site-specific deviation is represented by a depth Gaussian Process (depth-GP) acting on the residuals of the latent log-scale function. Differences between the measured and hierarchical-predicted UCS values are mapped into $\delta(z)$ along depth, enabling the model to start detecting whether the target site tends to produce higher or lower strengths than expected. Because of the spatial distribution of the available local data, a downward shift in the

UCS trend is observed, while the hierarchical predictor continues to provide stabilizing estimates within the upper 15m.

In Scenario C (i.e. 30% local data, Figure 6c), a larger portion of the target-site UCS observations is incorporated. The depth-GP now infers a clearer pattern of systematic site-specific deviation, producing a posterior profile that closely tracks local empirical evidence.

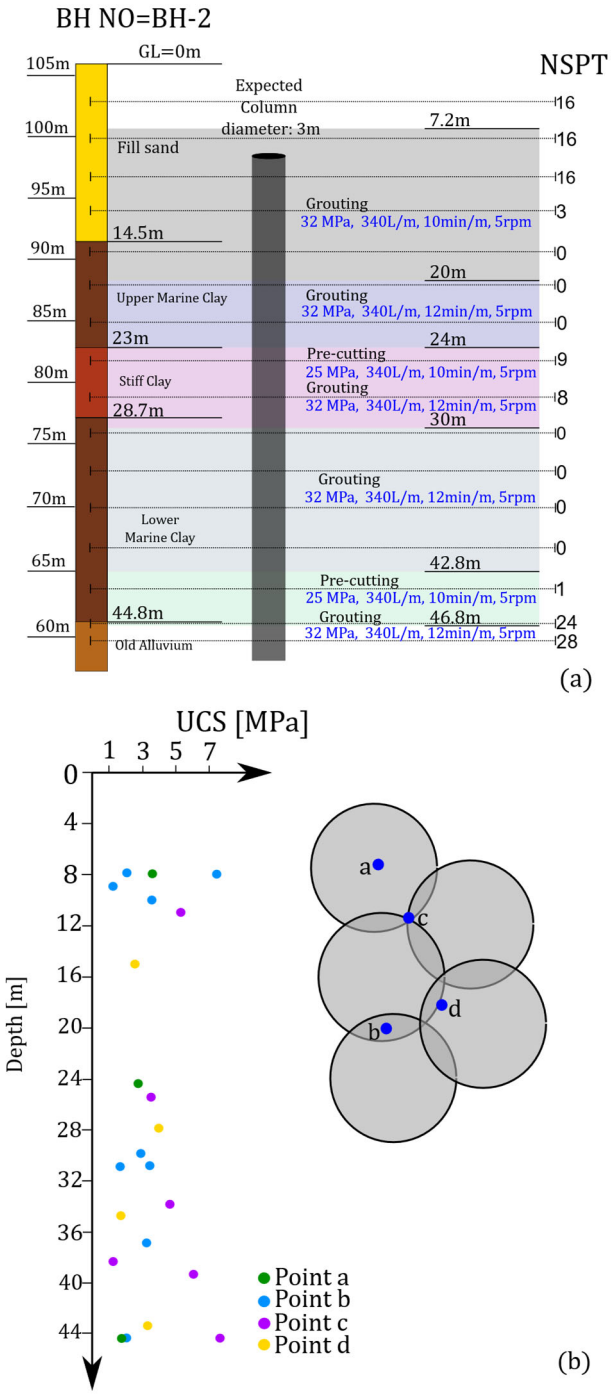

Figure 5. a) Project site lithology, jet-system parameters employed at different depths and N_{SPT} vertical profile. b) UCS measurements from laboratory tests (after Iwakubo et al., 2019).

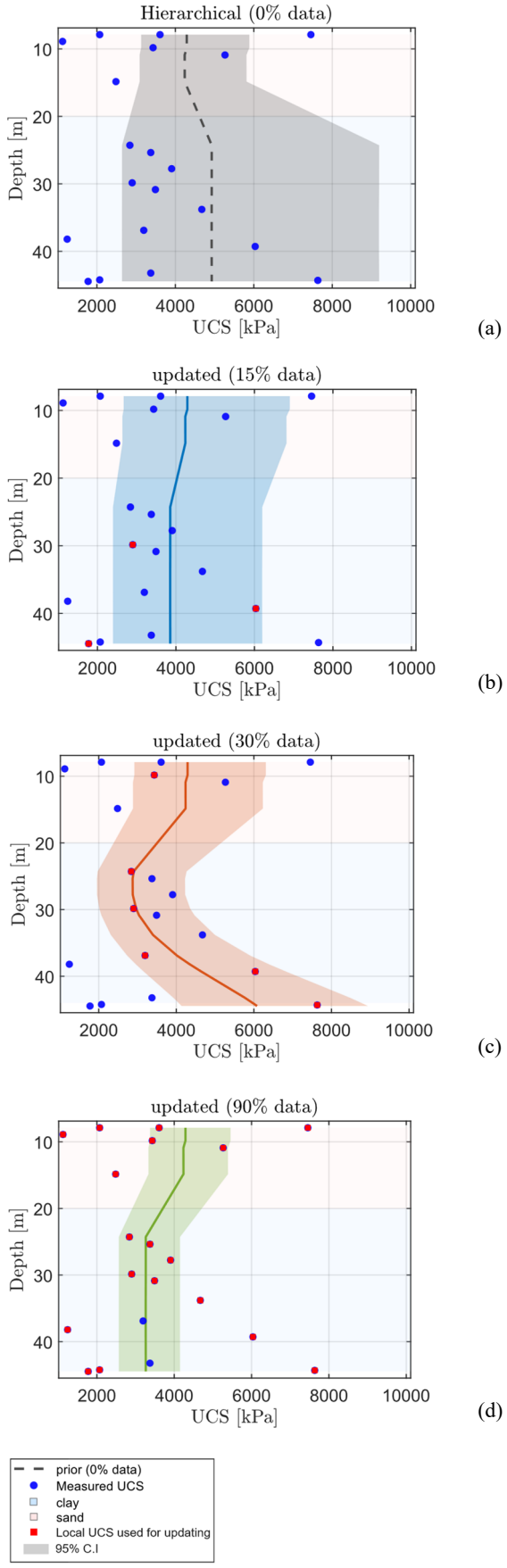

Figure 6. Target-site UCS spatial variability for different scenarios: a) No local data. b) 15% of local data. c) 30% of local data. d) 90% of available local data.

Finally, Scenario D (i.e. 90% of local data, Figure 6d), corresponds to nearly complete availability of local UCS measurements. The posterior UCS variability becomes almost entirely target-site driven. The local depth GP acts as a smooth interpolant of local measurements, while the hierarchical GP contributes mild regularization. Because the latent log-scale deviations are strongly constrained by abundant local observations, the posterior uncertainty strongly reduces, yielding a narrow confidence band. Overall, the four scenarios demonstrate the intended behavior of the hierarchical Weibull–GP model with site-level depth-GP updating. When data are scarce, predictions rely primarily on global and geological trends. As site data accumulates, the posterior UCS profile progressively adapts and ultimately converges to local trend spatial variability.

6 CONCLUSIONS

This paper presented a hierarchical Gaussian Process regression with a Weibull likelihood for predicting the unconfined compressive strength (UCS) of jet-grouted columns. The model integrates generic site information, geology-specific GPs, and a site-level depth-GP that updates predictions as local UCS measurements become available. This structure enables borrowing strength from past projects while preserving flexibility to adapt to project-site conditions, providing uncertainty-quantified UCS estimates even when only a few local data points exist. Application to a published case study demonstrated that the hierarchical model yields substantially improved predictive capabilities with respect to predictive models calibrated only on generic dataset. The four update scenarios showed smooth progression from dataset-dominated predictions (0 % of local data) to target-site-dominated UCS spatial variability (30 - 90% local data). For the specific case study, minimal site information (i.e. 15%) start reducing epistemic uncertainties while updating median trend variability. Moderate to dense local information (30–90%) produce narrow, realistic uncertainty bounds and good agreement with local observed UCS. These results highlight the value of hierarchical GP modelling for design-stage decision-making in jet grouting, offering a framework for UCS prediction and updating under limited local observations. Future work will extend the approach to multi-output prediction (i.e. including jet column diameter) and the assessment of clustering techniques in addition to the assumed coarse geological descriptors.

7 REFERENCES

Akan, R., Keskin, S.N., and Uzundurukan, S. 2015. Multiple regression model for the prediction of unconfined compressive strength of jet grout columns. *Procedia Earth and Planetary Science* 15, 299–303.

Ang, A.H.S., and Tang, W. H. 2007. *Probability Concepts in Engineering*. John Wiley.

Ching, J., Wu, S., and Phoon, K. K. (2021). Constructing quasi-site-specific multivariate probability distribution using hierarchical Bayesian model. *Journal of Engineering Mechanics*, *147*(10), 04021069.

Collico, S., Spagnoli, G., and Tintelnot, G. 2023. Statistical analysis of grouted tertiary sands with acrylate and polyurethane. *International Journal of Geosynthetics and Ground Engineering* 9(4), 41.

Collico, S., Spagnoli, G., and Kamata, T. 2025. A site-retrieval approach for the prediction of jet-grouted parameters. *Proceedings of ICE – Ground Improvement* 178(1), 279-292. https://doi.org/10.1680/jgrim.24.00069

Deisenroth, M., and Ng, J.W. 2015. Distributed Gaussian processes. In: *International Conference on Machine Learning*, 1481–1490. PMLR.

Díaz, E., Salamanca-Medina, E.L., and Tomás, R. 2024. Assessment of compressive strength of jet grouting by machine learning. *Journal of Rock Mechanics and Geotechnical Engineering* 16(1), 102–111.

Croce, P., Flora, A., and Modoni, G. 2014. *Jet Grouting*. CRC Press.

Ho, C.E. 2007. Fluid–soil interaction model for jet grouting. In: Hurley, T.M., and Johnsen, L.F. (eds), *Geo-Denver 2007*, 1–10. ASCE, Reston.

Iwakubo, T., Wong, R.K.N., Leong, G.K., Weng, Y.F., Chu, J., and Cheng, S.H. 2019. Performance of Rapid-Jet system for soil improvement works in soft marine clay. *TGS Special Publication*.

Modoni, G., Croce, P., and Mongiovì, L. 2006. Theoretical modelling of jet grouting. *Géotechnique* 56(5), 335–347.

Murphy, K.P. 2023. *Probabilistic Machine Learning: Advanced Topics*. MIT Press.

Nickisch, H., and Rasmussen, C. E. (2008). Approximations for binary Gaussian process classification. *Journal of Machine Learning Research*, *9*(10), 2035-2078.

Williams, C. K., and Rasmussen, C. E. (2006). *Gaussian processes for machine learning* (Vol. 2, No. 3, p. 4). Cambridge, MA: MIT Press.

Ribeiro, D., and Cardoso, R. 2017. A review on models for the prediction of the diameter of jet grouting columns. *European Journal of Environmental and Civil Engineering* 21(6), 641–669.

Shibazaki, M. 2003. State of practice of jet grouting. In: Johnsen, L.F., Bruce, D.A., and Byle, M.J. (eds), *Grouting and Ground Treatment*, 198–217. ASCE, Reston.

Spagnoli, G., and Oreste, P. 2025. Statistical interpretation of jet grouting field data regarding its strength and stiffness. *Geotechnical and Geological Engineering* 43, 44. https://doi.org/10.1007/s10706-024-03008-8.

Tinoco, J., Correia, A.G., and Cortez, P. 2014. Support vector machines applied to uniaxial compressive strength prediction of jet grouting columns. *Computers and Geotechnics* 55, 132–140.

Toraldo, C., Modoni, G., Ochmański, M., and Croce, P. 2017. The characteristic strength of jet-grouted material. *Géotechnique* 68, 262–279.

Wu, S., Ching, J., and Phoon, K.K. 2022. Quasi-site-specific soil property prediction using a cluster-based hierarchical Bayesian model. *Structural Safety* 99, 102253.

Yoshida, I., Tomizawa, Y., and Otake, Y. 2021. Estimation of trend and random components of conditional random field using Gaussian process regression. *Computers and Geotechnics* 136, 104179.

Zhang, L., Tang, W. H., Zhang, L., and Zheng, J. (2004). Reducing uncertainty of prediction from empirical correlations. *Journal of Geotechnical and Geoenvironmental Engineering*, *130*(5), 526-534.

Zhao, L.S., Qi, X., Tan, F., and Chen, Y. 2023. A new prediction model of the jet grouting column diameter for three jet grouting systems. *Computers and Geotechnics* 163, 105753.